Biochimica et Biophysica Acta 1848 (2015) 1277–1284

Contents lists available at ScienceDirect

Biochimica et Biophysica Acta

journal homepage: www.elsevier.com/locate/bbamem

Intramitochondrial accumulation of cationic Atto520-biotin proceeds via voltage-dependent slow permeation through lipid membrane

Yuri N. Antonenko [a,*], Natalya L. Nechaeva [b], Victoria E. Baksheeva [b], Tatyana I. Rokitskaya [a], Egor Y. Plotnikov [a], Elena A. Kotova [a], Dmitry B. Zorov [a]

[a] Belozersky Institute of Physico-Chemical Biology, Lomonosov Moscow State University, Moscow, Russian Federation
[b] Department of Bioengineering and Bioinformatics, Lomonosov Moscow State University, Moscow, Russian Federation

ARTICLE INFO

Article history:
Received 15 January 2015
Received in revised form 24 February 2015
Accepted 27 February 2015
Available online 6 March 2015

Keywords:
Rhodamine
Fluorescent dye
Penetrating cation
Mitochondria-targeted
Streptavidin
Fluorescence correlation spectroscopy

ABSTRACT

Conjugation to penetrating cations is a general approach for intramitochondrial delivery of physiologically active compounds, supported by a high membrane potential of mitochondria having negative sign on the matrix side. By using fluorescence correlation spectroscopy, we found here that Atto520-biotin, a conjugate of a fluorescent cationic rhodamine-based dye with the membrane-impermeable vitamin biotin, accumulated in energized mitochondria in contrast to biotin-rhodamine 110. The energy-dependent uptake of Atto520-biotin by mitochondria, being slower than that of the conventional mitochondrial dye tetramethyl-rhodamine ethyl ester, was enhanced by the hydrophobic anion tetraphenylborate (TPB). Atto520-biotin also exhibited accumulation in liposomes driven by membrane potential resulting from potassium ion gradient in the presence valinomycin. The induction of electrical current across planar bilayer lipid membrane by Atto520-biotin proved the ability of the compound to permeate through lipid membrane in a cationic form. Atto520-biotin stained mitochondria in a culture of L929 cells, and the staining was enhanced in the presence of TPB. Therefore, the fluorescent Atto520 moiety can serve as a vehicle for intramitochondrial delivery of hydrophilic drugs. Of importance for biotin-streptavidin technology, binding of Atto520-biotin to streptavidin was found to cause quenching of its fluorescence similar to the case of fluorescein-4-biotin.

1. Introduction

Mitochondrial dysfunction contributes to a wide range of pathologies including cardiovascular disorders, neurodegenerative diseases, diabetes, and cancer [1–3]. One of strategies of targeting therapeutic substances to mitochondria consists in covalent binding of a substance to a mitochondria-directed carrier representing a penetrating cation with a delocalized positive charge [1]. Accumulation of such cations, e.g. tetraphenylphosphonium, in mitochondria is driven by negative membrane potential on the inner mitochondrial membrane [4]. Since the pioneering work of Michael Murphy and co-authors describing the targeting of the antioxidant ubiquinone to mitochondria [5], this approach was successfully applied for intramitochondrial delivery of a mimetic of superoxide dismutase [6], the antioxidant plastoquinol [7], mild uncouplers quercetin [8] and fluorescein [9], imidazole-substituted fatty acids for inhibition of peroxidase activity [10], and others. Along with triphenylphosphonium, fluorescent carriers based on the derivatives of rhodamine 19 and rhodamine B were shown to deliver porphyrin and the antioxidant plastoquinol into mitochondria [11,12]. In the present study we demonstrate that the commercially available rhodamine 6G-related dye Atto520-biotin (Fig. 1), recently introduced for biotin-streptavidin technology, accumulates in mitochondria similar to other penetrating cations. Thus the cationic fluorescent moiety of Atto520 serves a role of a carrier for biotin facilitating its permeation through lipid membrane. Our finding of the accumulation of Atto520-biotin in mitochondria is unexpected because biotin, being rather hydrophilic, permeates poorly through lipid membrane [13]. In mammalian cells, the vitamin is transported across the plasma membrane by a sodium-dependent multivitamin transporter and, in some tissues, by a monocarboxylate transporter 1 [14]. In prokaryotes biotin is transported by the BioMNY system [15]. Of note, in cell death studies cell incorporation of NHS-biotin, a derivative of biotin with a capped carboxylic acid group, has been considered to indicate the loss of membrane integrity [16,17]. The present finding of the permeation of Atto520-biotin through mitochondrial membrane suggests that

Abbreviations: Atto520, a dye based on rhodamine 6G; TMRE, tetramethylrhodamine ethyl ester; TPB, tetraphenylborate; Stv, streptavidin; FCCP, carbonyl cyanide-p-trifluoromethoxyphenylhydrazone; DPhPC, diphytanoylphosphatidylcholine; FCS, fluorescence correlation spectroscopy; G(τ), autocorrelation function

* Corresponding author at: Belozersky Institute of Physico-Chemical Biology, Lomonosov Moscow State University, Moscow 119991, Russian Federation. Tel.: +7 495 939 51 49; fax: +7 495 939 31 81.
E-mail address: antonen@genebee.msu.ru (Y.N. Antonenko).

http://dx.doi.org/10.1016/j.bbamem.2015.02.028
0005-2736/

Atto520-biotin

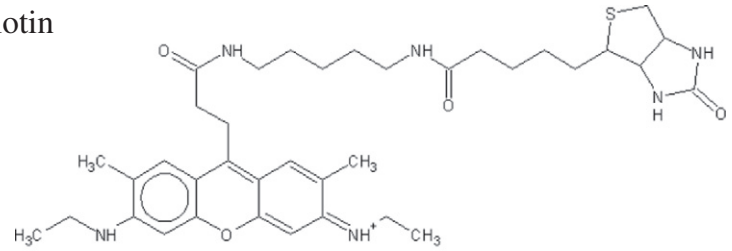

Biotin-rhodamine 110

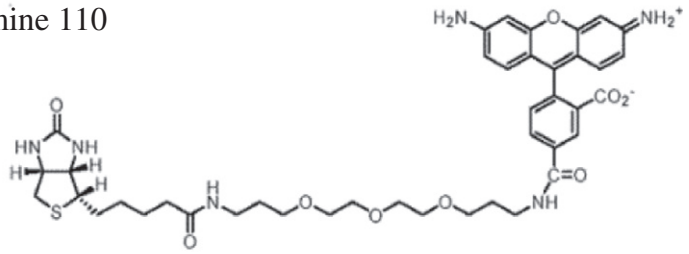

TMRE

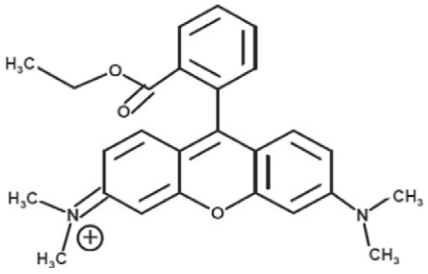

Fig. 1. Chemical structures of Atto520-biotin, biotin-rhodamine 110 and tetramethylrhodamine ethyl ester (TMRE).

voltage-dependent transmembrane diffusion of penetrating cations can be used for intramitochondrial delivery of hydrophilic compounds.

2. Materials and methods

Most chemicals were from Sigma; and succinate and sucrose were from ICN. Rhodamine 6G and TMRE (tetramethylrhodamine ethyl ester) were from Fluka. Atto520-biotin, fluorescein-4-biotin and streptavidin were from Sigma, and biotin-rhodamine 110 was from Biotium. Lipids of *Escherichia coli* were from Avanti polar lipids (Alabaster, Alabama).

2.1. Isolation of rat liver mitochondria

Rat liver mitochondria were isolated by differential centrifugation [18] in the medium containing 250 mM sucrose, 10 mM MOPS, 1 mM EGTA, and bovine serum albumin (0.1 mg/ml), pH 7.4. The final washing was performed in the same medium. Protein concentration was determined using bicinchoninic acid [19]. Handling of animals and experimental procedures were conducted in accordance with the international guidelines for animal care and use and were approved by the Ethics Committee of A. N. Belozersky Institute of Physico-Chemical Biology at Moscow State University.

2.2. Fluorescence correlation spectroscopy (FCS) experimental setup

FCS measurements were performed with a hand-made setup, as described previously in [20]. Briefly, fluorescence excitation and detection were provided by a Nd:YAG solid state laser with a 532-nm beam attached to an Olympus IMT-2 epifluorescence inverted microscope equipped with a 40×, NA 1.2 water immersion objective (Carl Zeiss, Jena, Germany). The fluorescence passed through an appropriate dichroic beam splitter and a long-pass filter and was imaged onto a 50-μm core fiber coupled to an avalanche photodiode (SPCM-AQR-13-FC, Perkin Elmer Optoelectronics, Vaudreuil, Quebec, Canada). The output signal F(t) was sent to a PC using a fast interface card (Flex02-01D/C, Correlator.com, Bridgewater, NJ). The signal was quantified in Hz meaning number of photons detected in a second. The data acquisition time *T* was 30 s. The experimental data were obtained under stirring conditions which increased the number of events by about three orders of magnitude thus substantially enhancing the resolution of the method. The card generated the autocorrelation function of the signal G(τ) defined as

$$G(\tau) = \frac{\langle \delta F(t) \cdot \delta F(t+\tau) \rangle}{\langle F(t) \rangle^2}$$

where <F(t)> is a mean fluorescence intensity and $\delta F(t) = F(t) - <F(t)>$ is a deviation from the mean. The $G(\tau)$ value in the limit of low τ was used for quantitative estimation of an average number of fluorescent particles, namely, for suspension of identical particles, according to [21]:

$$G(\tau \rightarrow 0) = \frac{1}{N}$$

where N is the average number of fluorescent particles in the confocal volume. Using this equation and knowing the mean signal of fluorescence of solutions of R6G, TMRE, or Atto520-biotin, one can estimate the brightness of the dyes in our FCS setup. The following values were derived for different dyes: rhodamine 6G, 1.35 kHz; Atto520-biotin, 0.95 kHz; TMRE, 0.37 kHz.

2.3. Treatment of the fluorescence signal (PIA procedure)

Fluorescence traces with sampling time of 25 μs were analyzed using the WinEDR Strathclyde Electrophysiology Software designed by J. Dempster (University of Strathclyde, UK). The software, originally designed for single-channel analysis of electrophysiological data, enables counting of the number of peaks ($n(F > F_0)$) of the FCS signal with amplitudes higher than the value F_0. A program of our own design with a similar algorithm (coined Saligat; provided on request) was also used.

2.4. Electrical current across planar lipid bilayers

Planar bilayer lipid membrane (BLM) was formed from a 2% solution of total lipids from *E. coli* (Avanti Polar Lipids, Alabaster, AL) in *n*-decane on a hole (diameter 0.8 mm) in a Teflon partition separating two compartments of a chamber containing aqueous buffer solutions [22]. The electric current (I) was recorded under voltage-clamp conditions. Voltage was applied to BLM with two Ag–AgCl electrodes placed on the opposite sides of the BLM. The current measured by a patch-clamp amplifier (OES-2, OPUS, Moscow) was digitized using an NI-DAQmx device (National Instruments, Austin, TX) and analyzed with a PC using WinWCP Strathclyde Electrophysiology Software also designed by J. Dempster.

2.5. Preparation of liposomes

Liposomes were prepared from lipids of *E. coli* in a solution containing 10 mM Tris, 10 mM MES, 100 mM KCl, pH 7.4 by extrusion through a 100-nm filter (Avanti Mini-Extruder). To monitor the uptake of Atto520-biotin or TMRE by liposomes upon the addition of valinomycin (5 nM), peaks of fluorescence were measured by FCS in the medium lacking potassium ions, i.e. 100 mM choline chloride, 3 mM Tris–HCl, pH 7.4.

2.6. Emission spectra of Atto520-biotin

The emission spectrum of Atto520-biotin (excitation at 490 nm) was measured with a Panorama Fluorat 02 spectrofluorimeter (Lumex, Russia).

2.7. Experiments with renal tubular epithelium cell cultures

Kidneys were excised aseptically from 3–7 day old rats, then homogenized and placed in balanced Hanks solution at pH 7.4. After several washes the dispensed tissue was placed in 0.1% collagenase and incubated for 20–30 min at 37 °C. Large pieces were removed, and cells were sedimented by gentle centrifugation (50 *g*) for 3 min. The pellet was resuspended in DMEM/F-12 1:1 containing 10% fetal calf serum and seeded in culture plates and glass-bottom dishes. Atto520-biotin solution was added to the cultured cells to concentration 500 nM and incubated for 60 min at 37 °C in DMEM/F-12 medium containing 10 mM Hepes-NaOH. Yielded cells were imaged with an LSM510 inverted confocal microscope (Carl Zeiss Inc., Jena, Germany). Analysis of fluorochrome incorporation was performed in glass-bottom dishes with excitation at 543 nm and emission collected at 560–590 nm. Images were processed using ImageJ software (NIH, Bethesda, MD, USA).

3. Results and discussion

FCS setup measures fluorescence from an observation volume with dimensions below 1 μm, i.e. enabling the detection of a signal from individual fluorescent particles (either molecules of a fluorophore or particles of mitochondria carrying a fluorophore). Fig. 2 shows recordings of Atto520-biotin (panel A) and TMRE (panel B) fluorescence measured in a suspension of rat liver mitochondria before (curve 1) and after (curves 2 and 3) the addition of succinate. TMRE is a cationic dye which was shown to accumulate electrophoretically in mitochondria [23,24]. Curves 2 and curves 3 were recorded 1 min and 9 min after the addition of succinate, respectively. In the case of TMRE, the amplitude of signal peaks was substantially lower without succinate than 1 min after its addition, which is in line with our previous results [20], corresponding to energy-dependent uptake of the penetrating cation TMRE by mitochondria. In contrast to TMRE, Atto520-biotin accumulation required more

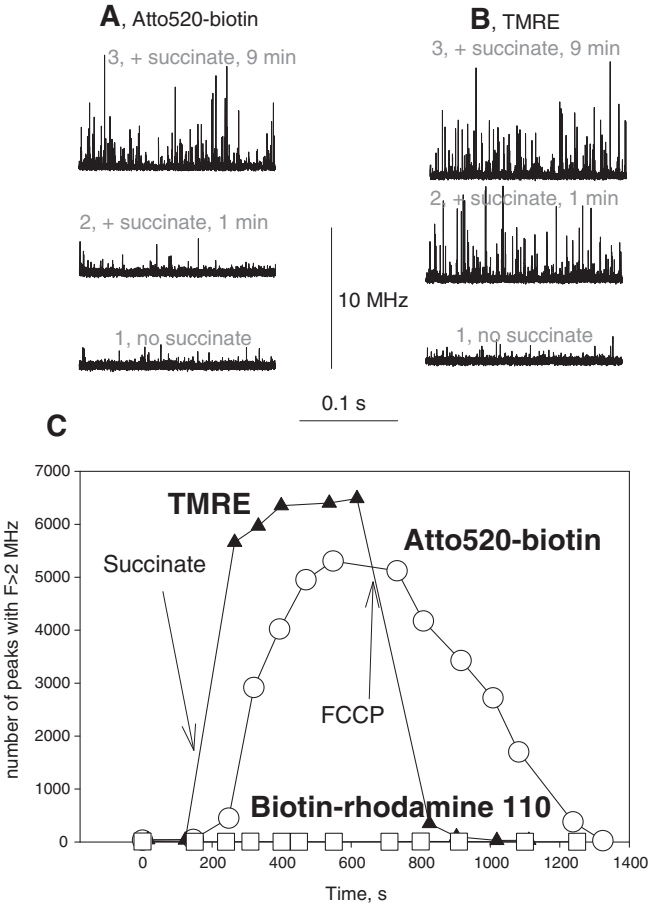

Fig. 2. A, B. FCS measurements of Atto520-biotin- and TMRE-uptake by mitochondria. Time-resolved count rates of Atto520-biotin (20 nM, panel A) and TMRE (20 nM, panel B) from a suspension of rat liver mitochondria in incubation buffer (0.1 mg protein/ml) in the absence (curve 1) and in the presence (curves 2 and 3) of 5 mM succinate, respectively. C. Kinetics of Atto520-biotin (open circles), TMRE (closed triangles) and biotin-rhodamine 110 (open squares) uptake by mitochondria upon their energization with succinate at t = 200 s. 1 μM FCCP was added at t = 700 s. The uptake was estimated as the number of peaks of fluorescence exceeding the amplitude of 2 MHz. Incubation mixture: 250 mM sucrose, 20 mM MOPS, 1 mM EGTA, 5 μM rotenone, 1 mg/ml BSA, pH 7.4.

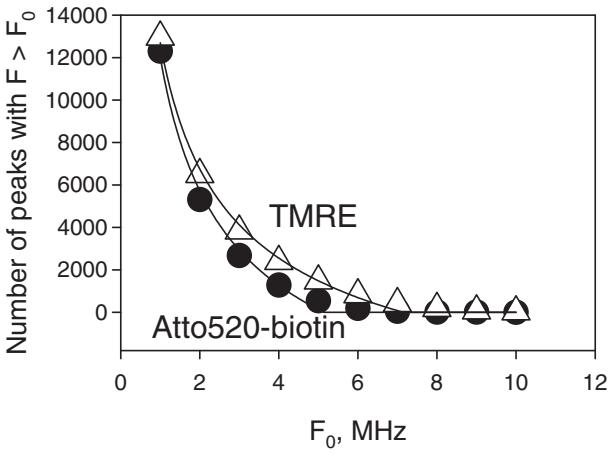

Fig. 3. Dependence of the number of peaks of fluorescence with $F > F_0$ on F_0 for Atto520-biotin (closed circles) and TMRE (open triangles) 15 min after the addition of succinate to mitochondria. Curves are best fits to Eq. (1) with mean fluorescence intensity per single mitochondron (parameter I_{single}) 5.1 MHz (Atto520-biotin) and 7.1 MHz (TMRE).

time to proceed and was well pronounced 9 min after the addition of succinate (Fig. 2B, curve 3).

Panel C of Fig. 2 shows the time courses of the dye accumulation using a parameter of n(F > 2 MHz), which is a number of peaks with an amplitude exceeding 2 MHz calculated during 30-s recording (X-axis shows the time of the end of each record). The kinetics of TMRE accumulation cannot be resolved by this approach because it is nearly completed 1 min after the addition of succinate (t = 180 s), or 2 min after the addition of the uncoupler FCCP (t = 700 s, closed triangles, Fig. 2C). In the case of Atto520-biotin, the kinetics of both accumulation and release were substantially slower and proceeded in the 10-min timescale (open circles, Fig. 2C). Fig. 2C also shows that biotin-rhodamine 110 exhibited no accumulation in contrast to TMRE or Atto520-biotin (open squares). This result could be expected because the molecule of rhodamine 110 is electrically neutral (a zwitter-ion, Fig. 1), which precludes its membrane potential-dependent inward transport.

The distribution of the number of peaks having different amplitudes (peak intensity analysis, PIA) for TMRE in the case of energized mitochondria differed only slightly from that of Atto520-biotin (Fig. 3 shows the data for t = 600 of Fig. 2). As shown in [20], the fitting of $n(F > F_0)$ by Eq. (1) can give a mean value of brightness of one stained mitochondrion (I_{single}):

$$n(F>F_0) = P_0 \cdot \left(\sqrt{\frac{I_{single}}{F_0}} - 1\right) \text{ for } F < I_{single}, \text{ and } n(F>F_0) = 0 \text{ for } F > I_{single}. \quad (1)$$

Curves in Fig. 3 showed best fits with the following parameters: I_{single} = 7.1 MHz (for TMRE), and 5.1 MHz (for Atto520-biotin). As it was described in the Materials and methods section, brightness of Atto520-biotin in our system exceeded that of TMRE by 2.5-fold suggesting that each mitochondrion accumulated a 3.5 times higher number of TMRE molecules than Atto520-biotin during 10 min of incubation with succinate. According to the description of the manufacturer, the fluorescence of Atto520-biotin decreased at pH > 7, which could affect the measurements of its accumulation into mitochondria by FCS because of the matrix alkalinization upon energization. However, our measurements showed that the reduction of Atto520-biotin fluorescence in the physiologically relevant range of pH from 7 to 9 is negligible (data not shown).

The protein streptavidin (Stv) is known to bind biotin very tightly, forming a membrane-impermeable complex. Fig. 4 displays the effect of Stv on the energy-dependent accumulation of Atto520-biotin. The addition of Stv after the accumulation (at t = 450 s) led to a slow release of Atto520-biotin from mitochondria (open circles, Fig. 4), while the addition of Stv prior to succinate prevented the accumulation (open squares, Fig. 4). Interestingly, the addition of Stv in combination with excess free biotin led to substantially less accumulation of Atto520-biotin compared to the control (closed squares, Fig. 4). This result could be associated with negative cooperativity in Atto520-biotin binding to Stv (having four biotin-binding sites), as suggested recently for fluorescein-4-biotin [25]. The effect of biotin could not be caused by putative uncoupling action of the compound because biotin by itself without Stv did not affect the accumulation of Atto520-biotin (closed circles, Fig. 4). This control experiment also highlighted the fact that Atto520-biotin accumulation proceeded without the involvement of protein transporters of biotin.

To exclude the possibility that the uptake of Atto520-biotin resulted from its binding to mitochondria rather than from its electrophoretic permeation through the inner mitochondrial membrane, we examined the effect of hydrophobic anions on the Atto520-biotin accumulation. Permeation of penetrating cations through lipid membranes is known to be accelerated by hydrophobic anions such as tetraphenylborate

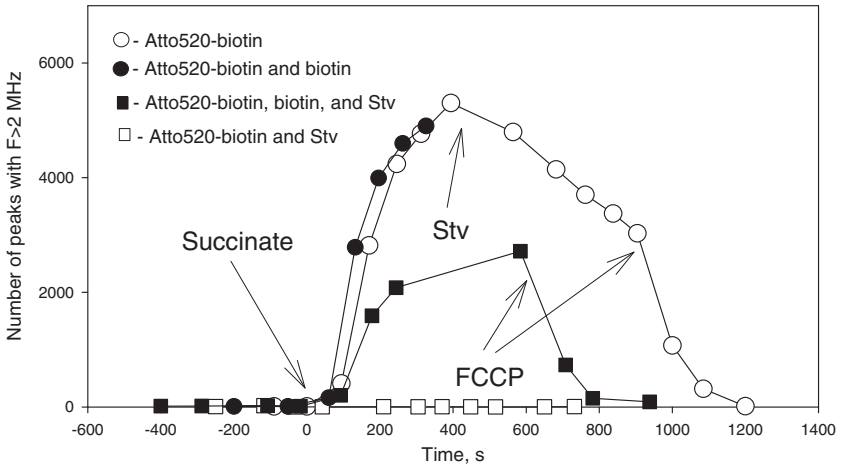

Fig. 4. Effect of streptavidin on the Atto520-biotin uptake by mitochondria upon their energization with succinate (5 mM) at t = 0 s. 1 μM FCCP was added where indicated. The uptake was estimated as the number of peaks of fluorescence exceeding amplitude of 2 MHz. Incubation mixture: 250 mM sucrose, 20 mM MOPS, 1 mM EGTA, 5 μM rotenone, 1 mg/ml BSA, pH 7.4. Stv, 6 μg/ml; biotin, 0.2 μM.

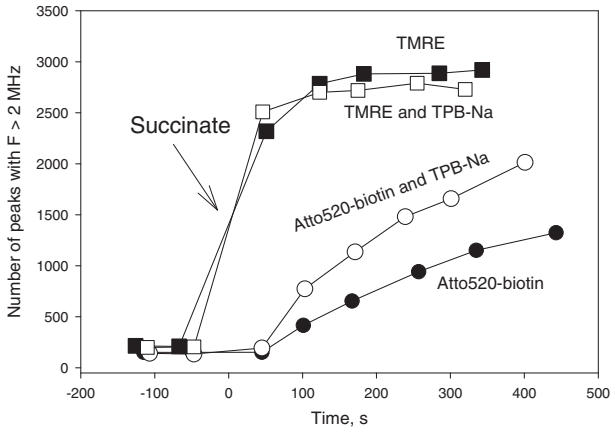

Fig. 5. Effect of sodium tetraphenylborate (TPB-Na) on the kinetics of Atto520-biotin (circles) and TMRE (squares) uptake by mitochondria upon their energization with succinate (5 mM) at t = 0 s. The uptake was estimated as the number of peaks of fluorescence exceeding amplitude of 2 MHz. Incubation mixture: 250 mM sucrose, 20 mM MOPS, 5 mM KH_2PO_4, 3 mM $MgCl_2$, 1 mM EGTA, 5 μM rotenone, 1 mg/ml BSA, pH 7.4. TPB-Na was 1 μM.

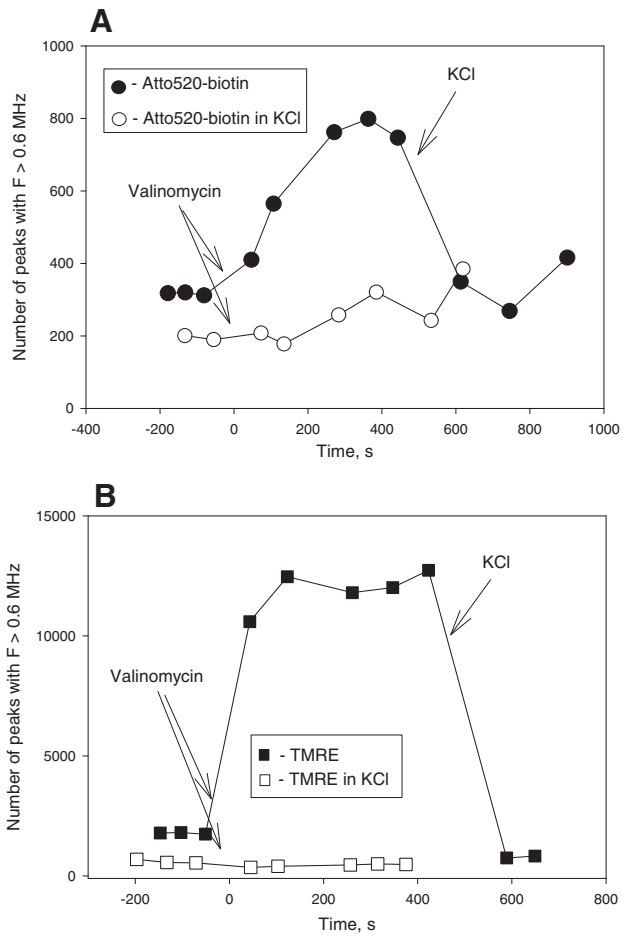

Fig. 6. Kinetics of Atto520-biotin (panel A, 20 nM, circles) and TMRE (panel B, 20 nM, squares) uptake by liposomes from *E. coli* lipids (20 μg/ml) upon the addition of valinomycin (5 nM at t = 0 s) in the presence of KCl gradient. KCl (100 mM) was added at t = 700 s. The uptake was estimated as the number of peaks of fluorescence exceeding amplitude of 0.6 MHz. Incubation mixture (closed symbols): 100 mM choline chloride, 1 μM TPB, 3 mM Tris–HCl, pH 7.4. Incubation mixture (open symbols): 100 mM KCl, 1 μM TPB, 3 mM Tris–HCl, pH 7.4.

(TPB) [26–28]. Actually, the initial rate of accumulation of Atto520-biotin was much faster in the presence of 1 μM TPB (Fig. 5, the curve with open circles), when compared to the control accumulation without TPB (closed circles). In contrast to TMRE, the steady-state levels of Atto520-biotin accumulation were not reached during these experiments. The kinetics of the TMRE uptake by mitochondria was too fast to be resolved in our system, whereas the steady-state level of TMRE reached after accumulation was not changed in the presence of TPB (Fig. 5, squares). Interestingly, the stimulation of Atto520-biotin accumulation by TPB was substantially lower than the stimulation of the accumulation of 1-methyl-4-phenylpyridinium observed in [26].

If the accumulation of Atto520-biotin in mitochondria was a result of voltage-dependent permeation of the cations through the membrane, it should also be observed in liposomes having electrical potential built by potassium ion gradient in the presence of the potassium ion carrier valinomycin. Liposomes in combination with the potential-sensitive dye DiS-C_3-5 represent a conventional system used for studying protonophores and ion channels [29]. Initially our FCS experiments did not reveal potential-dependent accumulation of Atto520-biotin in liposomes in contrast to the accumulation of TMRE (data not shown). However, in the presence of TPB (1 μM) the accumulation of Atto520-biotin was well pronounced (Fig. 6A, closed circles). Similar to the case of mitochondria, the accumulation of Atto520-biotin in liposomes was substantially lower, if compared to the accumulation of TMRE (Fig. 6B, closed squares). The kinetics of Atto520-biotin accumulation in liposomes was slow and lasted several minutes, while the accumulation of TMRE was fast and reached maximum after the first recording of the fluorescence. The addition of KCl led to efflux of both Atto520-biotin and TMRE from liposomes (marked by an arrow at t = 500 s, Fig. 6). Open circles and squares in Fig. 6 present control experiments in the KCl medium, i.e. without potassium ion gradient and thus without generated electric potential on the membrane of liposomes. As expected, the accumulation of the dyes was nulled under these conditions. Of note, there was significant accumulation of TMRE in liposomes even in the absence of valinomycin (closed squares in Fig. 6B) exceeding that in the presence of KCl (open squares in Fig. 6B). This result could be related to intrinsic potassium permeability of the liposomal membrane leading to the formation of some, albeit low, potential even without valinomycin.

Direct evidence of the permeation of the cationic form of Atto520-biotin could arise from measurements of electrical current through a planar bilayer lipid membrane (BLM), as it has been demonstrated for a series of penetrating cations [30,31]. Fig. 7 shows a comparison of the induction of electrical current through BLM by TMRE (panel A) and Atto520-biotin (panel B) upon the application of 150 mV at t = 0. Upper curves correspond to the experiments in the presence of phloretin which is known to decrease the dipole potential of lipid membranes stimulating permeation of cations and inhibiting permeation of anions [32,33]. In contrast to TMRE (Fig. 7), Atto520-biotin did not induce electrical current on BLM (the current was less than 2 pA which was close to a signal noise). However in the presence of phloretin, the Atto520-biotin-mediated BLM current amounted to about 40 pA, which was much larger than the resolution of the current measurement. Phloretin by itself did not induce the electrical current under the same conditions (data not shown). Besides establishing the stationary electrical current in the presence of phloretin, TMRE induced the characteristic current relaxation from the initial value of 160 pA to about 60 pA after 10–20 s. This demonstrates the increased binding of TMRE to the membrane–water interface in the presence of phloretin and its transmembrane redistribution upon voltage application. Thus, the data on BLM confirmed the ability of the cationic form of Atto520-biotin to permeate through lipid membranes upon application of electrical potential.

Atto520-biotin has been introduced relatively recently and the literature lacks information about the effect of Stv on the fluorescence of the dye. Stv has four high-affinity biotin-binding sites. Fig. 8 shows emission spectra of Atto520-biotin in the presence of increasing concentrations of Stv. The spectrum of Atto520-biotin has a maximum at

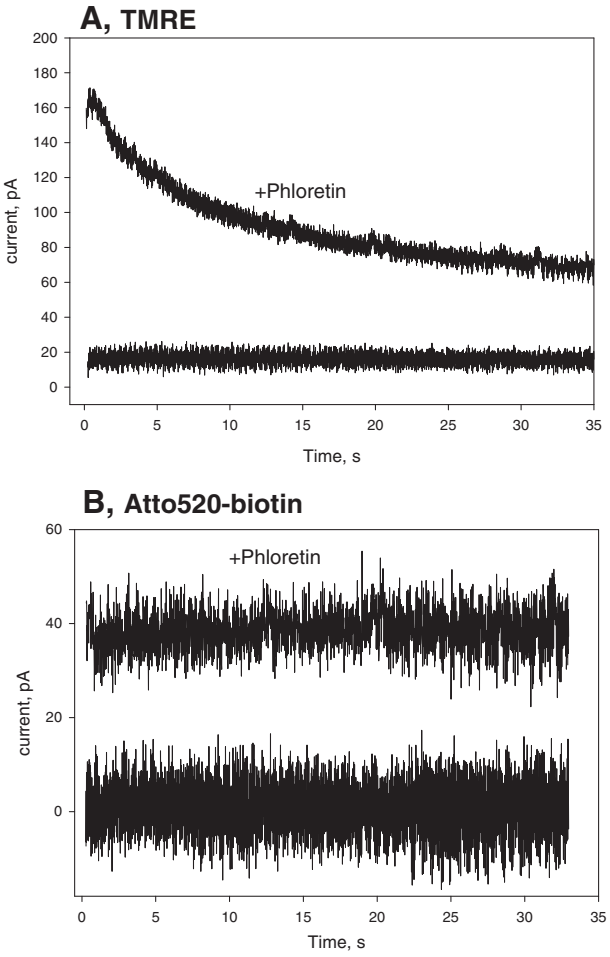

Fig. 7. Time courses of electrical current through BLM after application of voltage of $V = 150$ mV (at $t = 0$) in the presence of 1 μM of TMRE (panel A) or 0.5 μM Atto520-biotin (panel B) in the absence and in the presence of phloretin (5 μM). Planar phospholipid membrane was formed from *E. coli* lipids in decane. The solution contained 5 mM Tris, 5 mM MES, 100 mM KCl, pH 7.0.

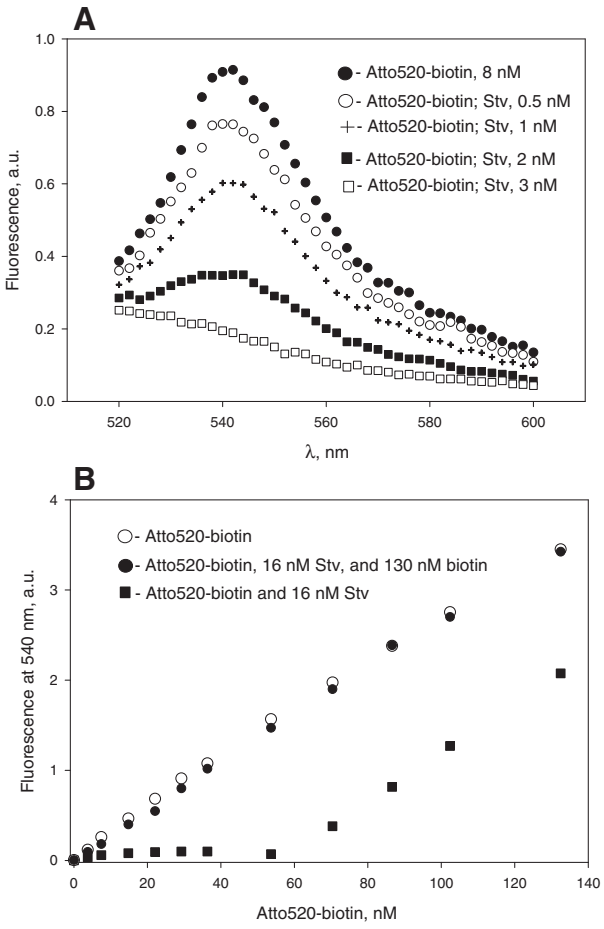

Fig. 8. Binding of Atto520-biotin to streptavidin. A. Effect of Stv on the emission spectra of Atto520-biotin (8 nM). Excitation, 490 nm. B. Dependence of Atto520-biotin fluorescence (excitation 490 nm, emission 540 nm) on its concentration in the absence and in the presence of 16 nM Stv. The solution was 100 mM KCl, 10 mM Tris, 10 mM MES, pH 7.0.

538 nm. As in the case of biotin-4-fluorescein [34], Stv quenched the fluorescence of Atto520-biotin (Fig. 8A) and the quenching was significant up to 4-fold excess of the dye over the protein (closed squares in Fig. 8B). At [Atto520-biotin]/[Stv] > 4 the fluorescence increased linearly with the concentration of Atto520-biotin (Fig. 8B). In the presence of an excess of biotin in the medium, the quenching of Atto520-biotin by Stv was absent (open and closed circles in Fig. 8B). Therefore, the behavior of Atto520-biotin fluorescence with respect to its interaction with Stv resembles that of fluorescein-4-biotin which is conventionally used for quantification of biotin-binding groups in different systems [35].

Confocal fluorescence microscopy of L929 cell culture revealed rather weak accumulation of Atto520-biotin in cells (Fig. 9). However, morphology of structures stained by Atto520-biotin suggests that it localized predominantly in mitochondria. Fig. 9A shows fluorescence images of cells after incubation with Atto520-biotin. As in the case of isolated mitochondria, it has been previously shown that accumulation of certain penetrating cations in cells is enhanced in the presence of the hydrophobic anion TPB [36]. Statistical analysis of confocal images (at least 10 fields of view per assay) shows an increase in fluorescence intensity of Atto520-biotin in the presence of 10 μM TPB, whereas 1 μM TPB was of no effect (Fig. 9D). Thus, TPB enhanced the accumulation of Atto520-biotin in mitochondria of cells suggesting the common mechanism with other penetrating cations.

Summarizing, it can be concluded that Atto520-biotin is accumulated in isolated energized mitochondria and mitochondria in situ by the mechanism typical for penetrating cations such as tetraphenylphosphonium, TMRE and others. The cationic Atto520 moiety exhibited the ability to play a role of a carrier for biotin. Low permeability of Atto520-biotin compared to TMRE could be attributed to hydrophilicity of biotin which itself is membrane-impermeable [13]. Interestingly, Atto520 was shown to be suitable for the super-resolution imaging of cells [37,38] suggesting that Atto520-biotin can be used for staining mitochondria in the STORM method.

In the present study we demonstrate that the addition of Stv prevents the energy-dependent accumulation of Atto520-biotin in mitochondria (Fig. 4). Apparently, this result implies that the benefit of the free energy of biotin binding to the protein exceeded free energy release upon the transfer of a positive charge through the inner mitochondrial membrane having a potential of about 180 mV [39]. This was not surprising because the affinity of biotin to streptavidin is exceptionally high reaching a value for a covalent bond [40]. It can be assumed that by using Stv mutants differing in the affinity to biotin, one can find a mutant unable to prevent the accumulation of Atto520-biotin in energized mitochondria, which can serve as a method to evaluate the mitochondrial membrane potential knowing the biotin-binding constant for this mutant protein. We believe that this approach can be of interest as an independent way to estimate the electrical potential on mitochondria because conventional measurements of this parameter are not

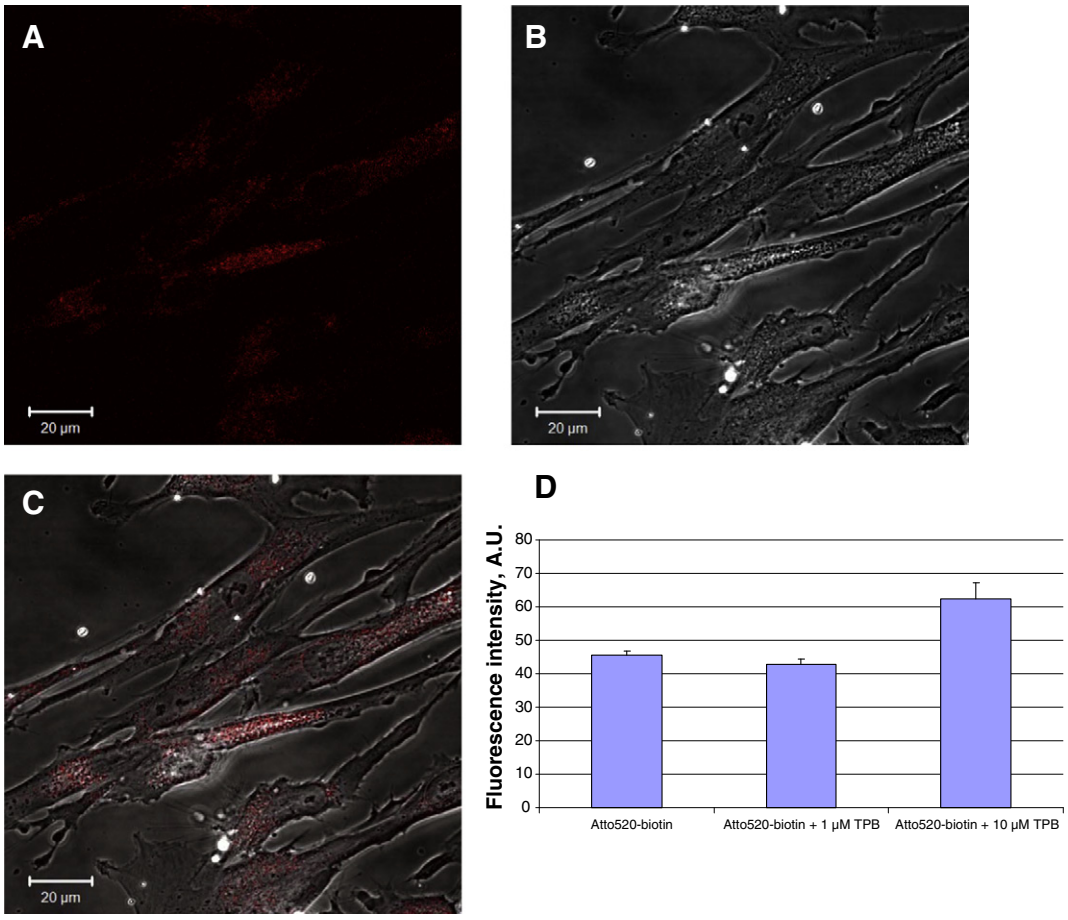

Fig. 9. Confocal fluorescence microscopy of L929 cells loaded with Atto520-biotin (A, red), phase contrast (B) and overlay (C). Panel D shows the effect of the hydrophobic anion TPB on the accumulation of Atto520-biotin.

devoid of drawbacks including energy-independent binding of penetrating cations to mitochondria.

Transparency Document

The Transparency document associated with this article can be found, in the online version.

Acknowledgements

We are grateful to Anna Lapashina for technical assistance. We are also thankful to Dr. Wladas Kozlovsky for improvement of the software support for the PIA method (program Saligat). This work was financially supported by the Russian Science Foundation (No. 14-24-00107).

References

[1] M.P. Murphy, R.A. Smith, Targeting antioxidants to mitochondria by conjugation to lipophilic cations, Annu. Rev. Pharmacol. Toxicol. 47 (2007) 629–656.
[2] F.M. Cunha, C.C. Caldeira da Silva, F.M. Cerqueira, A.J. Kowaltowski, Mild mitochondrial uncoupling as a therapeutic strategy, Curr. Drug Targets 12 (6) (2011) 783–789.
[3] V.P. Skulachev, V.N. Anisimov, Y.N. Antonenko, L.E. Bakeeva, B.V. Chernyak, V.P. Erichev, O.F. Filenko, N.I. Kalinina, V.I. Kapelko, N.G. Kolosova, B.P. Kopnin, G.A. Korshunova, M.R. Lichinitser, L.A. Obuchova, E.G. Pasyukova, O.I. Pisarenko, V.A. Roginsky, E.K. Ruuge, I.I. Senin, I.I. Severina, M.V. Skulachev, I.M. Spivak, V.N. Tashlitsky, V.A. Tkachuk, M.Y. Vyssokikh, L.S. Yaguzhinsky, D.B. Zorov, An attempt to prevent senescence: a mitochondrial approach, Biochim. Biophys. Acta 1787 (5) (2009) 437–461.
[4] E.A. Liberman, V.P. Skulachev, Conversion of biomembrane-produced energy into electric form. IV. General discussion, Biochim. Biophys. Acta 216 (1970) 30–42.
[5] G.F. Kelso, C.M. Porteous, C.V. Coulter, G. Hughes, W.K. Porteous, E.C. Ledgerwood, R.A. Smith, M.P. Murphy, Selective targeting of a redox-active ubiquinone to mitochondria within cells: antioxidant and antiapoptotic properties, J. Biol. Chem. 276 (2001) 4588–4596.
[6] A. Dhanasekaran, S. Kotamraju, C. Karunakaran, S.V. Kalivendi, S. Thomas, J. Joseph, B. Kalyanaraman, Mitochondria superoxide dismutase mimetic inhibits peroxide-induced oxidative damage and apoptosis: role of mitochondrial superoxide, Free Radic. Biol. Med. 39 (2005) 567–583.
[7] Y.N. Antonenko, A.V. Avetisyan, L.E. Bakeeva, B.V. Chernyak, V.A. Chertkov, L.V. Domnina, O.Y. Ivanova, D.S. Izyumov, L.S. Khailova, S.S. Klishin, G.A. Korshunova, K.G. Lyamzaev, M.S. Muntyan, O.K. Nepryakhina, A.A. Pashkovskaya, O.Y. Pletjushkina, A.V. Pustovidko, V.A. Roginsky, T.I. Rokitskaya, E.K. Ruuge, V.B. Saprunova, I.I. Severina, R.A. Simonyan, I.V. Skulachev, M.V. Skulachev, N.V. Sumbatyan, I.V. Sviryaeva, V.N. Tashlitsky, J.M. Vassiliev, M.Y. Vyssokikh, L.S. Yaguzhinsky, A.A. Zamyatnin Jr., V.P. Skulachev, Mitochondria-targeted plastoquinone derivatives as tools to interrupt execution of the aging program. 1. Cationic plastoquinone derivatives: synthesis and in vitro studies, Biochemistry (Mosc) 73 (2008) 1273–1287.
[8] L. Biasutto, N. Sassi, A. Mattarei, E. Marotta, P. Cattelan, A. Toninello, S. Garbisa, M. Zoratti, C. Paradisi, Impact of mitochondriotropic quercetin derivatives on mitochondria, Biochim. Biophys. Acta 1797 (2010) 189–196.
[9] S.S. Denisov, E.A. Kotova, E.Y. Plotnikov, A.A. Tikhonov, D.B. Zorov, G.A. Korshunova, Y.N. Antonenko, A mitochondria-targeted protonophoric uncoupler derived from fluorescein, Chem. Commun. 50 (2014) 15366–15369.
[10] J.F. Jiang, A. Bakan, A.A. Kapralov, K.I. Silva, Z.T. Huang, A.A. Amoscato, J. Peterson, V.K. Garapati, S. Saxena, H. Bayir, J. Atkinson, I. Bahar, V.E. Kagan, Designing inhibitors of cytochrome c/cardiolipin peroxidase complexes: mitochondria-targeted imidazole-substituted fatty acids, Free Radic. Biol. Med. 71 (2014) 221–230.
[11] Y.N. Antonenko, A.V. Avetisyan, D.A. Cherepanov, D.A. Knorre, G.A. Korshunova, O.V. Markova, S.M. Ojovan, I.V. Perevoshchikova, A.V. Pustovidko, T.I. Rokitskaya, I.I. Severina, R.A. Simonyan, E.A. Smirnova, A.A. Sobko, N.V. Sumbatyan, F.F. Severin, V.P. Skulachev, Derivatives of rhodamine 19 as mild mitochondria-targeted cationic uncouplers, J. Biol. Chem. 286 (2011) 17831–17840.
[12] E.J. Ngen, P. Rajaputra, Y. You, Evaluation of delocalized lipophilic cationic dyes as delivery vehicles for photosensitizers to mitochondria, Bioorg. Med. Chem. 17 (2009) 6631–6640.
[13] J. Rosenbluh, E. Hariton-Gazal, A. Dagan, S. Rottem, A. Graessmann, A. Loyter, Translocation of histone proteins across lipid bilayers and mycoplasma membranes, J. Mol. Biol. 345 (2005) 387–400.

[14] J. Zempleni, Uptake, localization, and noncarboxylase roles of biotin, Annu. Rev. Nutr. 25 (2005) 175–196.
[15] P. Hebbeln, D.A. Rodionov, A. Alfandega, T. Eitinger, Biotin uptake in prokaryotes by solute transporters with an optional ATP-binding cassette-containing module, Proc. Natl. Acad. Sci. U. S. A. 104 (2007) 2909–2914.
[16] U. Ziegler, P. Groscurth, Morphological features of cell death, News Physiol. Sci. 19 (2004) 124–128.
[17] C. Dumrese, C.F. Maurus, D. Gygi, M.K.J. Schneider, M. Walch, P. Groscurth, U. Ziegler, *Chlamydia pneumoniae* induces aponecrosis in human aortic smooth muscle cells, BMC Microbiol. 5 (2005) 2.
[18] D. Johnson, H. Lardy, Isolation of liver or kidney mitochondria, Methods Enzymol. 10 (1967) 94–96.
[19] P.K. Smith, R.I. Krohn, G.T. Hermanson, A.K. Mallia, F.H. Gartner, M.D. Provenzano, E.K. Fujimoto, N.M. Goeke, B.J. Olson, D.C. Klenk, Measurement of protein using bicinchoninic acid, Anal. Biochem. 150 (1985) 76–85.
[20] I.V. Perevoshchikova, D.B. Zorov, Y.N. Antonenko, Peak intensity analysis as a method for estimation of fluorescent probe binding to artificial and natural nanoparticles: tetramethylrhodamine uptake by isolated mitochondria, Biochim. Biophys. Acta 1778 (2008) 2182–2190.
[21] D. Magde, E.L. Elson, W.W. Webb, Fluorescence correlation spectroscopy. II. An experimental realization, Biopolymers 13 (1974) 29–61.
[22] P. Mueller, D.O. Rudin, H.T. Tien, W.C. Wescott, Methods for the formation of single bimolecular lipid membranes in aqueous solution, J. Phys. Chem. 67 (1963) 534–535.
[23] B. Ehrenberg, V. Montana, M.D. Wei, J.P. Wuskell, L.M. Loew, Membrane potential can be determined in individual cells from the nernstian distribution of cationic dyes, Biophys. J. 53 (1988) 785–794.
[24] D.L. Farkas, M.D. Wei, P. Febbroriello, J.H. Carson, L.M. Loew, Simultaneous imaging of cell and mitochondrial membrane potentials, Biophys. J. 56 (1989) 1053–1069.
[25] L. Li, J.O. Fierer, T.A. Rapoport, M. Howarth, Structural analysis and optimization of the covalent association between SpyCatcher and a peptide tag, J. Mol. Biol. 426 (2014) 309–317.
[26] G.P. Davey, K.F. Tipton, M.P. Murphy, Uptake and accumulation of 1-methyl-4-phenylpyridinium by rat-liver mitochondria measured using an ion-selective electrode, Biochem. J. 288 (1992) 439–443.
[27] G. Stark, Negative hydrophobic ions as transport-mediators for positive ions — evidence for a carrier mechanism, Biochim. Biophys. Acta 600 (1980) 233–237.
[28] Y.N. Antonenko, L.S. Khailova, D.A. Knorre, O.V. Markova, T.I. Rokitskaya, T.M. Ilyasova, I.I. Severina, E.A. Kotova, Y.E. Karavaeva, A.S. Prikhodko, F.F. Severin, V.P. Skulachev, Penetrating cations enhance uncoupling activity of anionic protonophores in mitochondria, PLoS ONE 8 (2013) e61902.
[29] T. Konishi, N. Murakami, Y. Hatano, K. Nakazato, Simultaneous determination of membrane-potential and pH gradient by photodiode array spectroscopy, Biochim. Biophys. Acta 862 (1986) 278–284.
[30] G.B. Melikyan, B.N. Deriy, D.C. Ok, F.S. Cohen, Voltage-dependent translocation of R18 and DiI across lipid bilayers leads to fluorescence changes, Biophys. J. 71 (1996) 2680–2691.
[31] T.I. Rokitskaya, S.S. Klishin, I.I. Severina, V.P. Skulachev, Y.N. Antonenko, Kinetic analysis of permeation of mitochondria-targeted antioxidants across bilayer lipid membranes, J. Membr. Biol. 224 (2008) 9–19.
[32] O.S. Andersen, A. Finkelstein, I. Katz, A. Cass, Effect of phloretin on permeability of thin lipid membranes, J. Gen. Physiol. 67 (1976) 749–771.
[33] E. Melnik, R. Latorre, J.E. Hall, D.C. Tosteson, Phloretin-induced changes in ion transport across lipid bilayer membranes, J. Gen. Physiol. 69 (1977) 243–257.
[34] G. Kada, H. Falk, H.J. Gruber, Accurate measurement of avidin and streptavidin in crude biofluids with a new, optimized biotin-fluorescein conjugate, Biochim. Biophys. Acta 1427 (1999) 33–43.
[35] A. Ebner, M. Marek, K. Kaiser, G. Kada, C.D. Hahn, B. Lackner, H.J. Gruber, Application of biotin-4-fluorescein in homogeneous fluorescence assays for avidin, streptavidin, and biotin or biotin derivatives, Methods Mol. Biol. 418 (2008) 73–88.
[36] R.E. Heikkila, J. Hwang, S. Ofori, H.M. Geller, W.J. Nicklas, Potentiation by the tetraphenylboron anion of the effects of 1-methyl-4-phenyl-1,2,3,6-tetrahydropyridine and its pyridinium metabolite, J. Neurochem. 54 (1990) 743–750.
[37] S. van de Linde, U. Endesfelder, A. Mukherjee, M. Schuttpelz, G. Wiebusch, S. Wolter, M. Heilemann, M. Sauer, Multicolor photoswitching microscopy for subdiffraction-resolution fluorescence imaging, Photochem. Photobiol. Sci. 8 (2009) 465–469.
[38] G.T. Dempsey, J.C. Vaughan, K.H. Chen, M. Bates, X.W. Zhuang, Evaluation of fluorophores for optimal performance in localization-based super-resolution imaging, Nat. Methods 8 (2011) 1027–1036.
[39] V.P. Skulachev, Transmembrane electrochemical H^+-potential as a convertible energy source for the living cell, FEBS Lett. 74 (1977) 1–9.
[40] T. Sano, S. Vajda, C.R. Cantor, Genetic engineering of streptavidin, a versatile affinity tag, J. Chromatogr. B 715 (1998) 85–91.